DESIGN OF AN INTENSE MUON SOURCE WITH A CARBON AND MERCURY TARGET

Diktys Stratakis, J. Scott Berg, BNL*, Upton, NY 11973, USA
David Neuffer, Fermilab†, Batavia, IL, USA
Xiaoping Ding, University of California, Los Angeles, CA, USA

Table 1: Parameters of the target and incident proton beam. Carbon target parameters are taken from [1], without the dump, with the target radius increased to 10 mm, and a corresponding increase in the proton beam size. For mercury, the target, proton beam, and solenoid axis lie in the same plane at the crossing point, with the proton beam to the outside. The optimization process for obtaining the target geometry is described in [2].

Material	C	Hg [3]
Target Radius (mm)	10.00	4.04
RMS Beam Size (mm)	2.5	1.212
Target Tilt (mrad)	65	127
Crossing Angle (mrad)	0	20.6
Proton Energy (GeV)	6.75	8
Geometric Emittance (μm)	5	0

Abstract

In high-intensity sources, muons are produced by firing high energy protons onto a target to produce pions. The pions decay to muons which are captured and accelerated. In the present study, we examine the performance of the channel for two different target scenarios: one based on liquid mercury and another one based on a solid carbon target. We detail the design and optimization o fhte system and its integration with the rest of the muon capture channel. With the aid of numerical simulations, we estimate the number of captured muons for the two different target concepts and specify the needed key lattice parameters such as the rf cavities, rf gradients, and solenoidal fields for each case.

PARTICLE DISTRIBUTIONS

We produce particle distributions from mercury and carbon targets under similar conditions. A proton beam hits a target, with the relevant parameters described in Table 1. The target is in a field that peaks near 20 T at the center of the beam-target crossing, and tapers down to 2 T just under 5 m downstream, and continues at that field downstream from that point. The solenoids that produce this field are described in Table 2; the choice of this field profile was based on [5]. A beam pipe with an inner radius of 13 cm surrounds the target and extends downstream to 85 cm from the beam-target crossing point. Downstream from there, the beam pipe has an inner radius of 23 cm. Particle production computations were performed using MARS15(2014) [6, 7].

Table 2: Solenoid coil geometries and currents [4].

Inner Radius (m)	Outer Radius (m)	Front Position (m)	End Position (m)	Current Density (A/mm^2)
0.160	0.208	−0.814	0.810	20.577
0.211	0.263	−0.814	0.810	17.503
0.267	0.323	−0.814	0.810	14.964
0.326	0.387	−0.814	0.810	12.855
0.390	0.456	−0.814	0.810	10.989
1.200	2.000	−2.017	1.378	19.098
1.200	1.791	1.378	2.198	21.103
1.200	1.230	4.581	6.214	43.579
1.200	1.251	6.340	6.563	43.249
1.200	1.238	6.615	7.179	43.643
1.200	1.235	7.258	9.402	43.332
1.200	1.360	9.520	9.670	42.882
1.000	1.160	10.330	10.480	42.882
1.000	1.035	10.630	14.400	42.882
1.000	1.160	14.550	14.700	42.882
1.000	1.160	15.330	15.480	42.882
1.000	1.035	15.630	19.430	42.882
1.000	1.160	19.580	20.180	42.882

We found that the choice of event generator parameters for nuclear inelastic interactions had a significant impact on particle production, as shown in Figs. 1 and 2. In contrast to [2, 3], but like [1], these studies use IQGSM=1, the current MARS15(2014) default [7]. Pion production per unit of proton power in mercury is notably higher than in carbon for lower pion energies, but the production rapidly becomes closer above 250 MeV (Figs. 3 and 4). The differences are much larger for negative than for positive pions. Thus the particle capture system should be optimized differently for a mercury than for a carbon target due to the lower-energy spectrum in mercury. Furthermore, the difference in the spectral shape between positive and negative pions in mercury requires that the optimal capture parameters for positive

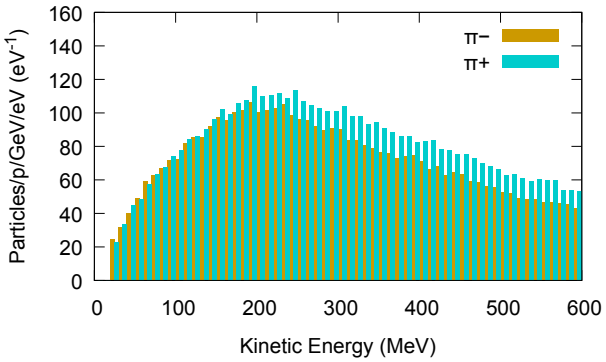

Figure 1: Pion spectrum from carbon, 2 m downstream from the beam-target crossing, with IQGSM=0 in MARS15(2014) [7], corresponding to the default value used in [2, 3].

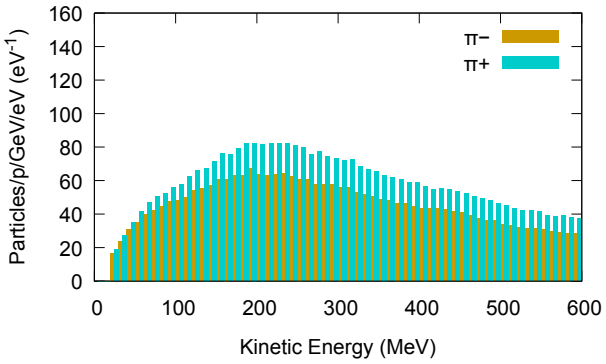

Figure 2: As in Fig. 1, but with IQGSM=1, the current MARS15(2014) default [7].

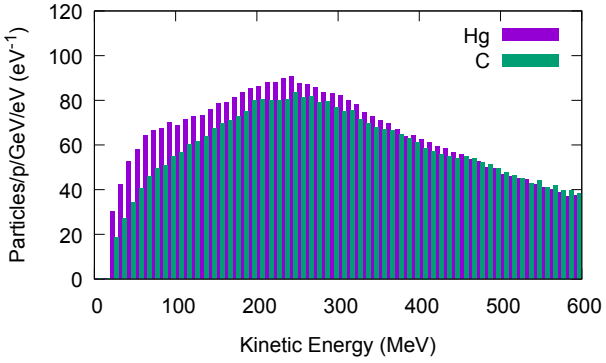

Figure 3: Distribution of positive pions 2 m downstream from the beam-target crossing point for a mercury target with an 8 GeV incident proton beam and a carbon target with a 6.75 GeV incident proton beam. Values are divided by proton beam energy in GeV and histogram bin width.

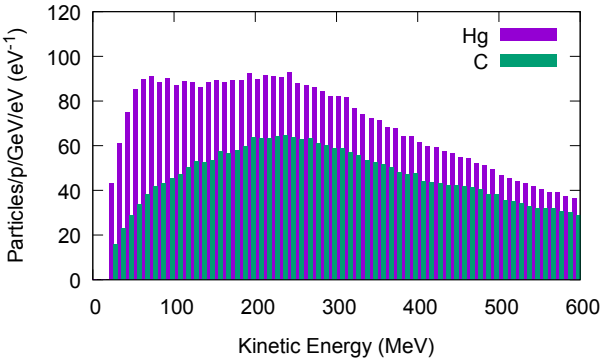

Figure 4: As in Fig. 3, but for negative pions.

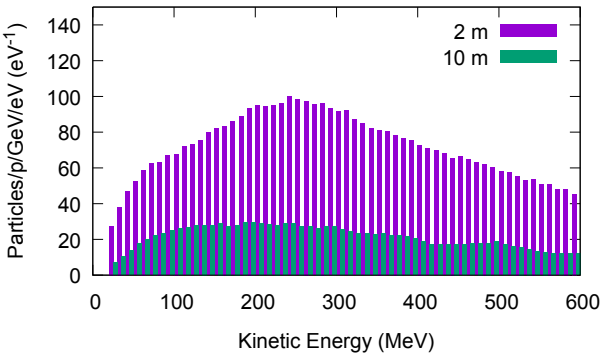

Figure 5: Positive pion spectra at two positions downstream from the beam-target crossing point.

and negative particles will be different, and some application-dependent opimal compromise parameters should be chosen. Large numbers of pions are lost on the beam pipe, with a greater fractional loss for higher energy pions (see Fig. 5, and note that the pion loss far exceeds the muon gain in Fig. 6). Thus a higher solenoid field downstream (giving a smaller beam size) will lead to more particles transmitted and ultimately captured (consistent with results in [5]), but the capture system will need to be retuned for a higher energy range to make optimal use of the increased field. Finally, we have inconclusive evidence that a small amount of absorber

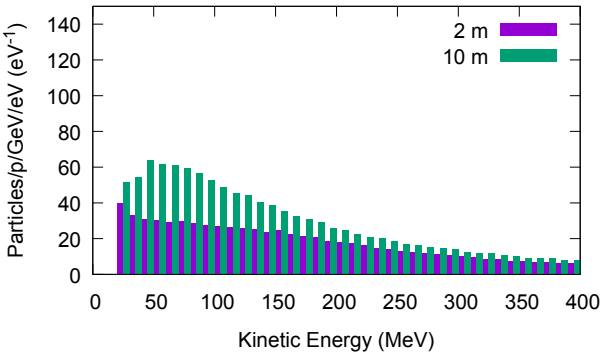

Figure 6: Positive muon spectra at two positions downstream from the beam-target crossing point.

at large radius may increase the number of particles in the low energy portion of the spectrum, potentially leading to improved performance.

REFERENCES

[1] X. Ding, H. G. Kirk, and K. T. McDonald. "Carbon Target Optimization for a Muon Collider/Neutrino Factory with a 6.75 GeV Proton Driver." In: *Proceedings of IPAC2014, Dresden, Germany*. Ed. by Christine Petit-Jean-Genaz et al. July 2014, pp. 3982–3984. ISBN: 978-3-95450-132-8. http://jacow.org/

[2] X. Ding et al. "Optimization of a Mercury Jet Target for a Neutrino Factory or a Muon Collider." In: *Physical Review Special Topics — Accelerators and Beams* 14 (Nov. 9, 2011), p. 111002. ISSN: 1098-4402. DOI: 10.1103/PhysRevSTAB.14.111002.

[3] X. Ding et al. "Gallium as a Possible Target Material for a Muon Collider or Neutrino Factory." In: *Proceedings of IPAC2012, New Orleans, Louisiana, USA*. IPAC'12 OC and IEEE, July 2012, pp. 232–234. ISBN: 978-3-95450-115-1. http://jacow.org/

[4] R. J. Weggel et al. "Magnet Design for the Target System of a Muon Collider/Neutrino Factory." In: *Proceedings of IPAC2014, Dresden, Germany*. Ed. by Christine Petit-Jean-Genaz et al. July 2014, pp. 3976–3978. ISBN: 978-3-95450-132-8. http://jacow.org/

[5] Hisham Kamal Sayed and J. Scott Berg. "Optimized Capture Section for a Muon Accelerator Front End." In: *Physical Review Special Topics — Accelerators and Beams* 17 (July 28, 2014), p. 070102. ISSN: 1098-4402. DOI: 10.1103/PhysRevSTAB.17.070102.

[6] Nikolai V. Mokhov. *The MARS Code System User's Guide Version 13(95)*. Physics Note FERMILAB-FN-628. Fermilab, Apr. 1995; O. E. Krivosheev and N. V. Mokhov. "Status of MARS Electromagnetic Physics." In: *Advanced Monte Carlo for Radiation Physics, Particle Transport Simulation and Applications. Proceedings of the Monte Carlo 2000 Conference, Lisbon, 23–26 October 2000*. Ed. by A. Kling et al. Fermilab Preprint FERILAB-Conf-00/181. Berlin and Heidelberg: Springer-Verlag, 2001, pp. 141–146. ISBN: 978-3-642-62113-0. DOI: 10.1007/978-3-642-18211-2_24; Nikolai V. Mokhov. *Status of MARS Code*. Preprint FERMILAB-Conf-03/053. Fermilab, Mar. 24, 2003; N. V. Mokhov et al. "Recent Enhancements to the MARS15 Code." In: *Radiation Protection Dosimetry* 116.1–4 (2005). Fermilab Preprint FERMILAB-Conf-04/053-AD, pp. 99–103. DOI: 10.1093/rpd/nci106. arXiv: nucl-th/0404084; Nikolai Mokhov. *MARS Code System*. Mar. 22, 2013. http://www-ap.fnal.gov/MARS/

[7] Nikolai V. Mokhov and Catherine C. James. *The MARS Code System User's Guide. Version 15(2014)*. May 8, 2014. http://www-ap.fnal.gov/MARS/